POLITYKA ENERGETYCZNA – ENERGY POLICY JOURNAL

2026 ✦ Volume 29 ✦ Issue 3 ✦ 59–80

DOI: 10.33223/epj/215271

Mohammed Mahmood Mustafa[1], Adnan M. Hussein[2], Afrah Turki Awad[3]

Enhancement of a spiral-tube PV/T collector using nanofluid under hot climatic conditions: experimental study

Abstract: This study experimentally investigates the performance of a spiral-tube photovoltaic/thermal (PV/T) collector integrated with single-crystal silicon PV modules and cooled using Al_2O_3/water nanofluid. Field trials were carried out in Kirkuk (Iraq) in March 2025 under operating conditions. A 0.5 wt% Al_2O_3 nanofluid was used as the working fluid, and its performance was compared to that of flat-plate PV panels under air-cooling conditions and modern water-cooled photovoltaic thermal (PV/T) configurations. 13:00, the nanofluid-cooled collector managed to maintain the PV cell at a minimum temperature of ~29°C, whereas the water-cooled and air-cooled panels were heated up to about 35°C and 60°C, respectively. Meanwhile, electrical efficiency at this time was 13.4% for the nanofluid-cooled PV/T, 12.6% for the water-block system, and 11.8% for the conventional PV module. The thermal efficiency of the nanofluid PV/T system was approximately 13%, while for water it was 12%. Note also that the net effectiveness was able to reach ~15.1% in the case of the nanofluid system and 14.5% for the water-cooled system. The results indicate that the nanofluid cooling effectively reduces PV cell temperature rise and thereby provides improved electrical, thermal, and overall performance in midday hot situations. In contrast to previous research under moderate weather and on

✉ Corresponding Author: Afrah Turki Awad; e-mail: afrah.turki@ntu.edu.iq

[1] Northern Technical University, Iraq; ORCID iD: 0009-0007-4598-3548; e-mail: mohammed.mahmood24gs@ntu.edu.iq)

[2] Northern Technical University, Iraq; ORCID iD: 0000-0001-6689-5423; e-mail: dradnan_hwj@ntu.edu.iq

[3] Northern Technical University, Iraq; ORCID iD: 0000-0003-3967-0821; e-mail: afrah.turki@ntu.edu.iq

flat plate PV/T systems, the current study experimentally illustrates the feasibility of reliable operation of a nanofluid-cooled spiral-tube PV/T collector in Iraq's intense heat.

Keywords: PV/T, spiral tube collector, Al_2O_3 nanofluid, PV cooling performance

Introduction

Sunlight is a renewable & environmentally friendly source of energy, and solar power is available in abundance. Solar energy is converted into electricity through the photoelectric effect by photovoltaic (PV) cells; however, a significant percentage of the incident energy is converted into heat instead of electricity (Faheem et al. 2024). This resulting excess heat increases the operating temperature of PV modules, which leads to an increase in the dark saturation current of the *p–n* junction owing to higher intrinsic carrier concentration (Abid et al. 2025). This, in turn, reduces open-circuit voltage and power performance, thereby inefficiency is low (Hasan et al. 2025). Furthermore, when it runs for long hours, excessive heat is considered not good for PV modules due to its reduction in their lifetime and durability (Hameed et al. 2024).

To overcome this problem, photovoltaic/thermal (PV/T) systems have been developed. In such systems, cooling fluid circulates through absorber tubes mounted behind the PV panel and carries off excess heat (ref.imachinery; Khaleel et al. 2025). Enhanced electrical efficiency, as well as useful thermal energy, can be recovered, e.g., for domestic hot water and space heating (Hosouli et al. 2024). PV/T collectors have better space-energy density and lower total cost than the separate PV and solar thermal systems (Mohammed et al. 2024; Shaalan et al. 2025a). Moreover, they are green, for their machine design is simple and can be embedded with buildings (Atyia and Qasim 2023; Awad and Hussein 2024).

PV/T collectors exist in a wide range of types, and working fluids among them include air, glycol, water, or refrigerants as heat extraction fluid (Pathak et al. 2022). For the water-type PV/T systems, these are the mass flow rate of water, the channel geometry, tube spacing along with local weather conditions (Dubey and Tiwari 2008). Generally, these systems show electrical efficiency of 10–12% and thermal efficiencies ranging between 33% and 72%, as reported previously (Kalogirou et al. 2016). Kalogirou et al. (2016) and Alhussen and Hussein (2024a) indicated that water-based PV/T systems performance can be classified as the sheet-and-tube, channel, free-flow, and two-absorber designs (Shaalan et al. 2025b). Air-based PV/T systems are generally single-pass or double-pass systems with electrical efficiencies of ca. 8% and thermal efficiencies >39% (Akrouch et al. 2023).

Other constructions have also been investigated and enumerated (Alhussen and Hussein 2024b; Ghadikolaei 2021). Although good heat transfer effects are achieved, traditional passive cooling methods experience both insufficient cooling power under peak solar radiation and non-uniform temperature distributions (Wang et al. 2022). Phase change materials (PCM) have been explored mainly because of their amount of absorbed and released latent heat during a phase transition (Awad et al. 2025). Organic PCMs such as paraffin wax and fatty acids, inorganic salt hydrates, and eutectic mixtures have been tested (Awad and Waleed 2023). Despite their potential, PCMs also present drawbacks such as toxicity, corrosiveness, and high material costs, which have limited their widespread use (Awad et al. 2021).

In recent years, the processing of solar energy systems using nanotechnology-based techniques has been an increasing concern and a promising solution to optimize the performance of these devices, such as with nanofluids. Suspensions of solid particles (smaller than 100 nm) in a base fluid, e.g., water, present an opportunity for enhancing the effective thermal conductivity and convective heat transfer significantly. This makes them particularly well suited for application to solar thermal collectors and PV/T hybrid systems, which require effective cooling under high levels of solar radiation. Water-based nanofluid offers cooling to decrease the temperature of a PV cell, which counterbalances the drop in electrical efficiency with temperature and increases both thermal and overall efficiencies. Table 1: To clearly position the present study, Table 1 briefly summarizes the recently used experimental studies of nanofluid-cooled photovoltaic/thermal (PV/T) collectors Nanofluid type Concentration Collector configuration Qyyum et al., and the associated improvements in electrical and thermal performance.

Table 1. Summary of recent studies on PV/T collectors using nanofluids

Tabela 1. Podsumowanie najnowszych badań dotyczących kolektorów PV/T wykorzystujących nanofluidy

Study/Year	Nanofluid	Conc./ Conditions	Collector type	Electrical eff. gain	Thermal/ Temp. effect	Notes
Murtadha and Hussein 2022	Al_2O_3/water	0.2–0.6%	One-pass PV/T	+2.5% (abs.)	Overall eff. 25%	Same nanofluid, higher conc.
Aydın et al. 2022	Al_2O_3/water	—	Flat-plate PV/T	Not reported	Thermal eff. +15.9–39.8%	Compared with water
Ibrahim et al. 2023	Al_2O_3/water	0.05 vol%, 0.07 kg/s	Serpentine PV/T	(reported avg. elec. eff. = 12.156% baseline)	Cell cooling 20 °C	Uncooled case 75.5°C
Lima-Téllez et al. 2024	Al_2O_3 (simulation)	10 vol%	Single-channel PV/T	+4% (abs.)	Cell temp dropped 15%	Numerical study
Srimanickam et al. 2025	Al_2O_3/water	—	Flat-plate PV/T	+12.4% (abs.)	Thermal 18.7%	Experimental + ML approach

To enable a fair and repeatable comparison with previous studies, Table 1 was organized using a single set of reporting criteria. Electrical gains are given as absolute percentage-point (pp) increases relative to each study's baseline PV/PV/T configuration, while thermal performance is reported as thermal efficiency (%) or as the reduction in cell temperature (°C), when available. For every study, we list the nanofluid type and concentration, mass flow rate, collector geometry (e.g., flat-plate, serpentine/spiral), and testing conditions (laboratory vs. field; moderate vs. hot climate. This unified format reduces ambiguity, aligns the definitions used across different sources, and allows direct comparison with the performance metrics adopted in the present work (η_e, η_{th}, η_o, and ΔT_{cell}).

Building on the studies summarized in Table 1, we defer the detailed validation of our findings against this literature to a dedicated subsection (validation with literature) placed after the Results and Discussion. This structure avoids redundancy and allows a direct, metric-by-metric comparison once our results have been fully presented.

Therefore, the objective of this study is threefold: (i) quantify cell-temperature reduction and electrical gains via a spiral-tube PV/T collector; (ii) assess the influence of Al_2O_3/water on thermal and overall performance; and (iii) benchmark nanofluid-cooled PV/T against conventional PV and water-cooled PV/T under identical outdoor conditions.

The novelty of this work lies in part in conducting an outdoor experimental investigation for a spiral-tube PV/T collector using Al_2O_3/water nanofluid as a cooling medium under the hot semi-arid region of Kirkuk, Iraq. Unlike in most prior work, the system is tested in direct comparison to an uncooled PV module as well as a water-cooled PV/T collector under identical operation conditions, enabling the strict separation of the effect of nanofluid cooling and spiral-tube geometry. The findings measure the effect of nanofluid application on the temperature of PV cells and on their electrical, thermal, and total efficiencies under high noon irradiance conditions. The study framework is proposed to be expanded in order to conduct a brief comparison between Al_2O_3/water and TiO_2/water as alternative nanofluid coolants for the practical consideration of choosing a type of nanofluids in PV/T applications under extreme climatic conditions.

1. Experimental setup and measurements

1.1. PV/T collector design

The experimental system employed a spiral-tube photovoltaic/thermal (PV/T) panel with overall dimensions of 2,280 × 1,130 × 35 mm. A copper spiral tube with an 15 mm outside diameter (OD) and 14 mm inside diameter (ID) was bonded to the back of a single-crystal silicon PV module, which was used as a heat exchanger. The system included a 6-liter storage container connected to both ends of the tube. The tank and piping network were designed to allow closed-loop circulation of the cooling fluid. Figure 1 shows a schematic of the spiral tube PV/T solar collector and its major components.

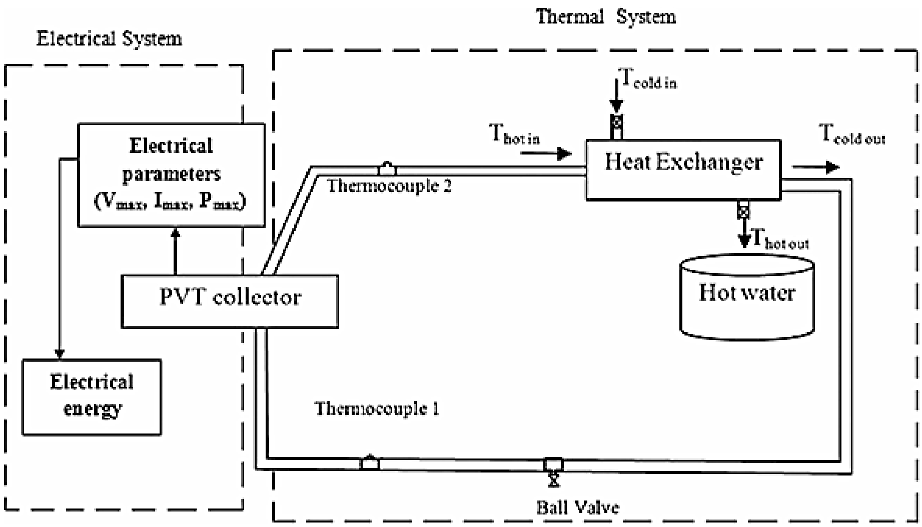

Fig. 1. Schematic diagram of the spiral-tube PV/T experimental setup and main components.

Rys. 1. Schemat eksperymentalnej konfiguracji PV/T z rurą spiralną oraz jej głównych elementów

1.2. Hydraulic circuit and operation

The storage system consisted of two tanks: one containing the working fluid (water or Al_2O_3 nanofluid) and the other acting as a coolant reservoir. Heat transfer between the two tanks was facilitated through a heat exchanger, maintaining thermal equilibrium. Flow through the spiral-tube PV/T collector was driven by thermosiphon and regulated at the inlet using a throttling valve. A sampling tap enabled timed volumetric collection of the working fluid; the measured volume per time was then converted to mass flow rate using the fluid density at the test temperature. Over the test window, the average flow was $\dot{m} =$ 0.07 kg/s (4.2 L/min at 25°C). This thermosiphon-based procedure ensures reproducible flow reporting without active pumping.

1.3. Test site and conditions

The studies were conducted at the Renewable Energy Research Center-Northern Technical University, Kirkuk, Iraq (35.39764° N, 44.34435° E). The solar radiation in the region is approximated at around 5.8 kWh/m^2/day year-round. The data were collected in March 2025 from 08 h to 17 h under a clear sky. Both the PV and PV/T systems were mounted with a fixed tilt angle of 30° towards the south. Figure 2 shows the experimental setup prototype.

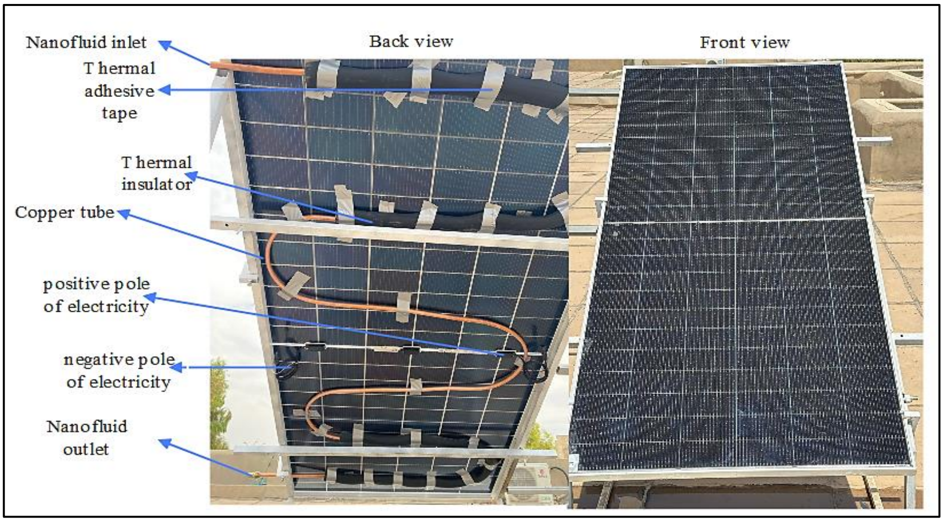

Fig. 2. Photograph of the spiral-tube PV/T experimental prototype installed at the Renewable Energy Research Center in Kirkuk, Iraq

Rys. 2. Zdjęcie eksperymentalnego prototypu kolektora słonecznego typu PV/T z rurą spiralną, zainstalowanego w Centrum Badań nad Energią Odnawialną w Kirkuku w Iraku

1.4. Instrumentation and measurements

- Solar radiation was measured using a calibrated solar power meter with an accuracy of ±10 W/m^2.
- PV module and absorber plate temperatures were recorded with K-type thermocouples (accuracy ±2.2°C).
- Surface temperatures were cross-checked using an infrared thermometer (accuracy ±2°C).
- Fluid inlet and outlet temperatures were measured simultaneously with thermocouples.
- Mass flow rate was quantified by timed volumetric collection at a sampling tap and converted to mass units using the fluid density at the test temperature; average $\dot{m}$ = 0.07 kg/s (4.2 L/min at 25°C).

1.5. Uncertainty analysis

An uncertainty analysis was conducted following standard procedures. Table 2 lists a summary of the estimated errors on the main parameters; The overall experimental uncertainty was estimated to be within ±5%, confirming the reliability of the obtained results.

TABLE 2. Uncertainty of parameters

TABELA 2. Niepewność parametrów

Parameter	Instrument	Accuracy	Uncertainty [%]
Solar radiation [W/m^2]	Solar power meter	±10 W/m^2	1.5
PV/plate temperature [°C]	K-type thermocouples	±2.2°C	3.5
Surface temperature [°C]	Infrared thermometer	±2°C	3.0
Mass flow rate [kg/s]	Volumetric measurement	±0.01 L/s	4.0

2. Electrical and thermal performance evaluation

2.1. Electrical efficiency

Different load resistance values will give different levels of voltage and current, and by substituting the test data into Equation (1), we can find out the maximum power point.

$$P_{\max} = V_{\max} \cdot I_{\max} \tag{1}$$

Here, $P_{\max}$, $V_{\max}$, and $I_{\max}$ denote the maximum power output voltage, and current. Simultaneous tests for both PV and PV/T systems are carried out every hour from 08:00 to 17:00 h. The same equivalent solar radiation intensities are measured. All measurements were made in March 2025 at noon when the sun was directly above. The efficiency can be found from Equation (2).

$$\eta_e = \frac{P_{max}}{G \cdot A} \tag{2}$$

where:

G – intensity of solar insolation [W/m^2],

A – panel area [m^2].

2.2. Temperature and thermal efficiency

Absorber temperatures of the PV/T system and PV panel are recorded at hourly reading, and daily during 08:00 h–17:00 h. Utilize at the same time input and output temperatures of the liquid. Then to determine the thermal efficiency.

$$\eta_{th} = \frac{mC_p\left(T_o - T_i\right)}{G \cdot A} \tag{3}$$

Here, $\dot{m}$ is the mass flow rate measured by volume and converted to the test temperature using density.

Fluid flow rate is represented by m [kg/s], specific heat of the fluid by C_p [J/kg·K], and T_o and T_i [°C] the input and output thermal energy.

2.3. Overall efficiency

Photovoltaic and PVT panels will have medium electrical efficiency. The total efficiency of a PV/T system is obtained by summing its thermal efficiency and average electrical efficiency. As can be seen from the equation, a compound system increases efficiency by making full use of solar energy in the same space.

$$\eta_o = \eta_e + \eta_{th} \tag{4}$$

where:

η_o, η_e, η_{th}– overall efficiency, photovoltaic (PV) efficiency, and thermal efficiency, respectively.

For many parameters, the hourly values are stored and plotted over time. We make findings by contrasting the results we got simultaneously for pure and PV/T panels. So by substituting those numbers into Equations (2) and (3), we can determine the electrical or thermal efficiency of the panels.

3. Nanofluid preparation and properties

3.1. Nanofluid preparation

At the nano level, particles of 10^{-9} meters – which can be manipulated through the use of nanotechnology – create nanoparticles. Alumina and titania are a couple of materials with relatively good thermal conductivities that can be milled into small nanoparticles (Najim et al. 2022). By adding nanoparticles to the base fluids (nucleate, convecting, or radiated) for heat transfer, a stable colloidal solution is produced. They are capable of enhancing the thermal conductivity of base fluids when mixed with base fluids, even if the base fluids have a low thermal conductivity (Rahman et al. 2024). This combination, which is called nanofluid, has been an emerging technology (Shaalan et al. 2025a). Nanofluid increases the heat transfer performance, which contributes to reducing the amount of large-sized heat exchange equipment (Muayad et al. 2025). Nanoparticles in nanofluids are solid particles that are as small as the colloidal particle sizes and that become adsorbed to each other by a special motion of the base fluid. As such, they are very efficient carriers of heat and conductors (Abdullah and Hussein 2023). The perfect colloidal suspension of nanoparticles should involve both homogeneous distribution and excellent stability (Khlaief et al. 2025).

In this work, a 0.5 wt% Al_2O_3/water nanofluid was prepared by the two-step method, which is commonly employed because of its simplicity and low cost. Commercial aluminum oxide nanopowder (< 50 nm average particle size, purity 99.9%, Sigma-Aldrich, USA) was employed as the dispersed phase, and deionized water (DIW) was used as the base fluid.

The weight fraction was estimated using the standard weight fraction formula. 35.78 g of Al_2O_3 nanopowder was added dropwise into 7.155 L of deionized water with magnetic stirring at room temperature (25°C) for 60 min, when the rotating speed reached 500 rpm. The suspension was sonicated (sonicator 40 kHz; 200 W) for 90 minutes, crashing the agglomeration to achieve uniform nanoparticle dispersion. No surfactant was used in order not to change the thermal conductivity of the nanofluid. Figure 3 represents the procedure of nanofluid preparation.

Here is the actual calculation on that. All the accounting runs through, as given: water level in a 6 L tank, 6.88 m copper pipe, and joining pipes; we have determined that we have 1.15 liters of water in each of the pipes. A 0.5% powder-to-water ratio was used in this experiment.

$$m_p = \frac{\varnothing \cdot \rho_p \cdot \left(\frac{m_f}{\rho_f} \right)}{(1 - \varnothing)} \tag{5}$$

Fig. 3. Preparation steps of the Al_2O_3/water nanofluid (magnetic stirring and ultrasonic dispersion)

Rys. 3. Etapy przygotowania nanofluidu Al_2O_3/woda (mieszanie magnetyczne i dyspersja ultradźwiękowa)

3.2. Thermophysical properties

The most critical property of HTFs is their thermal conductivity, which directly affects the heat transfer efficiency. Besides, nanofluids are found to be better than pure base fluids because of their high thermal conductivity, which can improve the heat transfer coefficient overall and lead to enhancement in PV/T systems performance. It can be observed that small particle size will lead to a higher thermal conductivity, which mitigates heat concentration and makes the stored energy easier to dissipate. On other hand, density and specific heat of nanofluids have impact on the performance in terms of storage and transport of energy; viscosity influences pumping power required and Reynolds number of flow among others. Hence, an overall assessment of the properties of a nanofluid is necessary when considering the performance of PV/T collectors. Thermophysical properties of the base fluid (water) and alumina nanoparticle are given in Table 3.

The thermophysical properties of the 0.5 wt% Al_2O_3/water nanofluid were estimated by standard correlations in this study at a reference temperature of 25°C and are tabulated as measured/calculated values (Table 4).

The governing equations used to calculate these properties are listed below:

Thermal Conductivity for Maxwell (Maxwell 2011):

$$k_{nf} = \frac{k_p + 2k_f + 2\varphi\left(k_p - k_f\right)}{k_p + 2k_f - \varphi\left(k_p - k_f\right)} k_f \tag{6}$$

Table 3. Thermophysical properties of base fluid (water) and Al_2O_3 NP

Tabela 3. Właściwości termofizyczne płynu bazowego (wody) i nanocząstek Al_2O_3

Property	Water	Al_2O_3	Unit
Density (ρ)	998.2	3,970	kg/m^3
Specific heat capacity (C_p)	4,179	765	J/kg·K
Thermal conductivity (k)	0.61	40	W/m·K
Dynamic viscosity (μ)	0.890	–	mPa·s

Source: Eisapour et al. 2020; Hissouf et al. 2020; Jia et al. 2020.

Table 4. Thermophysical properties of nanofluid

Tabela 4. Właściwości termofizyczne nanofluidu

Component	Wt%	Volume fraction Ø [%]	Density ρ [kg/m^3]	Specific heat C_p [J/kg·K]	Thermal conductivity k [W/m·K]	Dynamic viscosity (μ) [mPa·s]
Al_2O_3/water	0.5	0.126	1,002.0	4,174.7	0.6122	0.8928

Viscosity for Einstein (Einstein 1906):

$$\mu_{eff} = \mu(1 + 2.5\varphi)\varphi < 0.05 \tag{7}$$

Specific Heat for Pak and Cho (Pak and Cho 1998):

$$\rho_{nf} = \varphi\rho_p + (1-\varphi)\rho_{bf} \tag{8}$$

Density for Pak and Cho (Pak and Cho 1998):

$$C_{p,nf} = (1-\varphi)C_{p,bf} + \varphi C_{p,np} \tag{9}$$

4. Results and discussion

Figure 4 illustrates the hourly variation of electrical efficiency (η_e) for the three systems tested during March 2025. The general trend shows that the nanofluid-cooled PV/T collector consistently outperformed both the water- and air-cooled panels throughout the day. This improvement is mainly attributed to the enhanced heat transfer and better temperature regulation provided by the Al_2O_3/water nanofluid. At 08:00, during the early morning when ambient temperature was still low, the nanofluid system already exhibited a high electrical efficiency of about 13.9%, followed by 13.2% for the water-cooled PV/T and 12.0% for the air-cooled module. By 13:00, as the cell temperature rose due to peak solar loading, efficiencies slightly decreased for all systems; however, the nanofluid-cooled panel maintained the highest value of around 13.4%, compared with 12.6% and 11.8% for the water- and air-cooled configurations, respectively. Later in the afternoon, at 17:00, when both solar radiation and cell temperature declined, the efficiencies of all systems improved again, reaching approximately 13.8%, 12.5%, and 11.9% for the nanofluid, water, and air-cooled panels, respectively. Overall, the figure clearly demonstrates the stability and superior performance of the nanofluid-cooled PV/T collector under varying operating conditions.

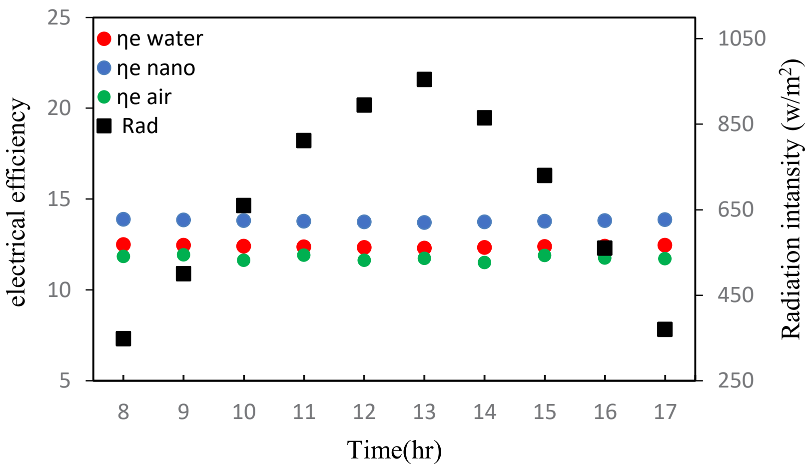

Fig. 4. Hourly variation of electrical efficiency for the uncooled PV module, water-cooled PV/T collector and Al_2O_3/water nanofluid-cooled PV/T collector during a clear day in March 2025

Rys. 4. Zmiany sprawności elektrycznej w ujęciu godzinowym dla modułu fotowoltaicznego bez chłodzenia, kolektora fotowoltaiczno-termicznego chłodzonego wodą oraz kolektora fotowoltaiczno-termicznego chłodzonego nanofluidem Al_2O_3/woda w pogodny dzień w marcu 2025 roku

Figure 5 illustrates the hourly variation of PV cell temperature for the three systems tested during March 2025. The overall pattern shows that the nanofluid-cooled collector maintained the lowest cell temperature at all times of the day, followed by the water-cooled PV/T, while the air-cooled module consistently exhibited the highest values. This is an indication of the better heat-transfer performance of Al_2O_3/water nanofluid and its ability to dissipate accumulated heat on the PV surface. At 08:00, the nanofluid system started at a low temperature (approximately 24°C) in contrast with the water-cooled panel (28°C) and the air-cooled PV (approximately

44°C). At 13:00, due to the increasing ambient temperature and solar loading, the differences between these three systems were further increased: about 29°C of nanofluid-cooled collector, approximately 35°C of water-cooled panel, and about 60°C of air cooler panel.

In the late afternoon, at 17:00, the temperatures of all systems declined as solar intensity decreased; the nanofluid panel cooled back to approximately 22°C, the water-cooled to 26°C, and the air-cooled to 38°C. The consistent temperature gap across the day confirms the superior cooling performance of the Al_2O_3/water nanofluid and its role in minimizing thermal stress on the PV cells.

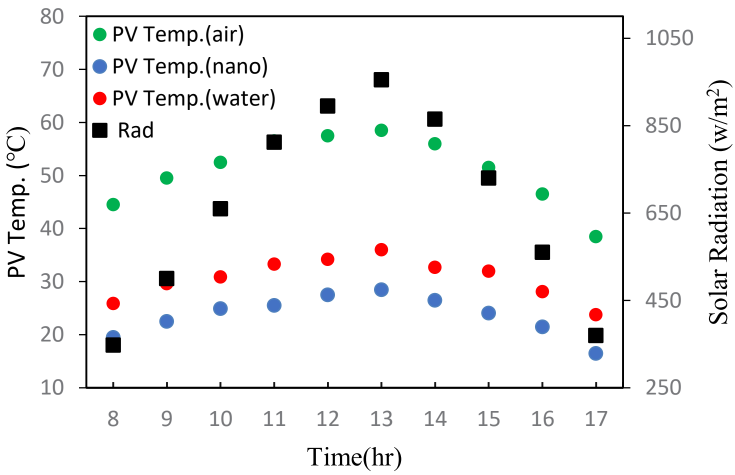

Fig. 5. Hourly variation of PV module back-surface temperature for the uncooled PV module, water-cooled PV/T collector and Al_2O_3/water nanofluid-cooled PV/T collector during a clear day in March 2025

Rys. 5. Zmiany temperatury tylnej powierzchni modułu fotowoltaicznego w ujęciu godzinowym dla modułu fotowoltaicznego bez chłodzenia, kolektora fotowoltaiczno-termicznego chłodzonego wodą oraz kolektora fotowoltaiczno-termicznego chłodzonego nanofluidem Al_2O_3/woda w pogodny dzień w marcu 2025 roku

Figure 6 illustrates the thermal efficiency (η_{th}) of the PV/T system cooled by Al_2O_3/water nanofluid compared with the water-cooled configuration. The overall pattern shows that thermal efficiency followed the typical daily behavior of solar collectors, starting high in the morning, decreasing gradually at midday, and recovering slightly in the late afternoon. This variation is mainly controlled by the temperature difference between the fluid inlet and outlet and the corresponding heat-transfer rate through the absorber. At 08:00, when both ambient and cell temperatures were relatively low, the nanofluid-cooled PV/T system achieved its highest thermal efficiency of about 20%, while the water-cooled collector recorded approximately 18%. By 13:00, as the outlet temperature of the working fluid increased, the temperature difference across the heat exchanger decreased, leading to lower efficiencies of around 13% for the nanofluid and 12% for water. In the late afternoon, at 17:00, as the system cooled and the temperature gradient increased again, thermal efficiency improved slightly, reaching 16% for the nanofluid and 15% for the water-cooled configuration. The results confirm that the Al_2O_3/water nanofluid enhances heat extraction during the morning and stabilizes system performance under high-temperature conditions.

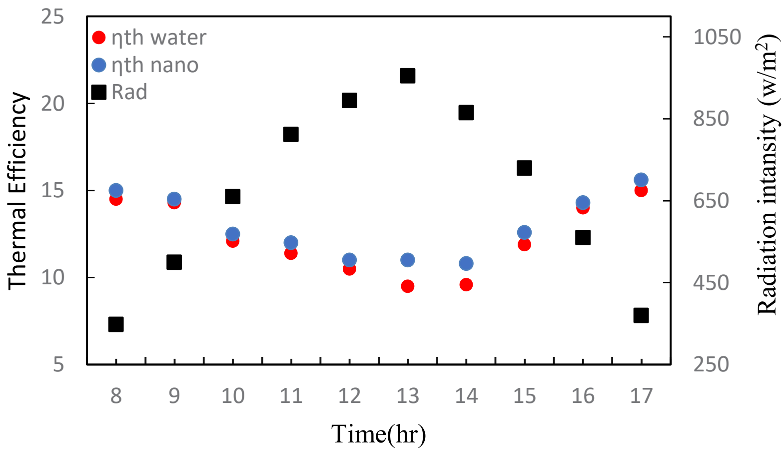

Fig. 6. Hourly variation of thermal efficiency for the water-cooled and Al_2O_3/water nanofluid-cooled PV/T collectors during a clear day in March 2025

Rys. 6. Zmiany sprawności cieplnej w ujęciu godzinowym dla kolektorów PV/T chłodzonych wodą oraz nanofluidem Al_2O_3/woda w pogodny dzień w marcu 2025 roku

Figure 7 tracks how the outlet temperature of the working fluid changed when the PV/T system operated with plain water and with the Al_2O_3/water nanofluid in March 2025. In both cases, the temperature rose gradually during the morning, reached a maximum around midday, and then dropped again toward the end of the day. Throughout the test hours, the nanofluid outlet temperature stayed slightly below that of water, which is consistent with its higher thermal conductivity and more effective heat transfer. At 08:00, the outlet temperature was about 22°C for the nanofluid and 23°C for water. Around 13:00, both fluids reached their peak values, roughly 27°C for the nanofluid and 28°C for water, showing that heat was being absorbed and carried away from the collector surface. By 17:00, as solar irradiance declined, the outlet temperatures fell to approximately 21°C for the nanofluid and 22°C for water. Even though the numerical difference between the two fluids is small, the consistently lower outlet temperature of the nanofluid indicates better heat removal and a more responsive thermal behavior of the PV/T system.

As can be seen from the above, the total system efficiency (η_o) is presented in Figure 8 for a PV/T area based on water and Al_2O_3/water nanofluid. It measures the electric and thermal output contribution, thus offering an overall figure of merit for system performance at various operating conditions. They show that the nanofluid-cooled collector generated a higher overall

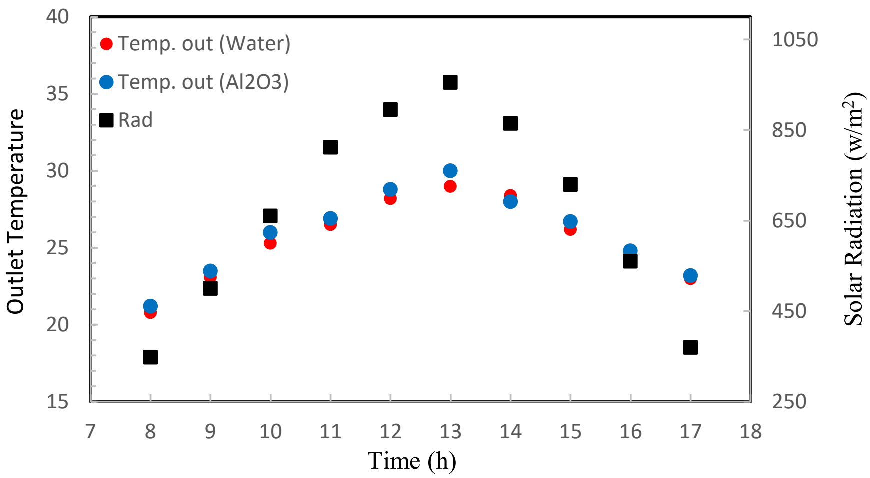

Fig. 7. Hourly variation of outlet fluid temperature for the water-cooled and Al_2O_3/water nanofluid-cooled PV/T collectors during a clear day in March 2025

Rys. 7. Zmiany temperatury płynu na wylocie w poszczególnych godzinach dla kolektorów PV/T chłodzonych wodą oraz nanofluidem Al_2O_3/woda w pogodny dzień w marcu 2025 roku

efficiency than the water-cooled system during all testing hours, indicating the positive thermal-electrical synergy of the nanofluid cooling. At 08:00, the total performance of nanofluid-modified PV/T was nearly 15.4%, and that for the water-cooled case was 14.8%. By 13:00, when the irradiance and PV cell temperature were relatively high, overall efficiency slightly decreased in both systems due to inferior thermal performance, but the nanofluid collector still had a higher value, with a percentage of approximately 15.1%, while water was at about 14.5%. In the late afternoon, at 17:00, as the panels cooled and the temperature gradient increased again, the overall efficiency recovered slightly, reaching nearly 15.6% for the nanofluid and 14.9% for the water-based system. This consistent improvement throughout the day demonstrates the effectiveness of Al_2O_3 nanofluid in enhancing total energy utilization and maintaining stable PV/T performance under real outdoor conditions.

Figure 9 presents the hourly overall efficiency of the PV/T collector when operated with water and with a TiO_2/water nanofluid, together with the corresponding solar radiation intensity. In order to extend the scope of the study, the system was additionally tested using TiO_2/water as a working fluid under the same operating and climatic conditions as those adopted previously for water and Al_2O_3/water. The results show a consistent improvement in overall efficiency with the TiO_2 nanofluid relative to water over the entire test period, indicating that the use of metal-oxide nanofluids can further enhance the energetic performance of the spiral-tube PV/T collector.

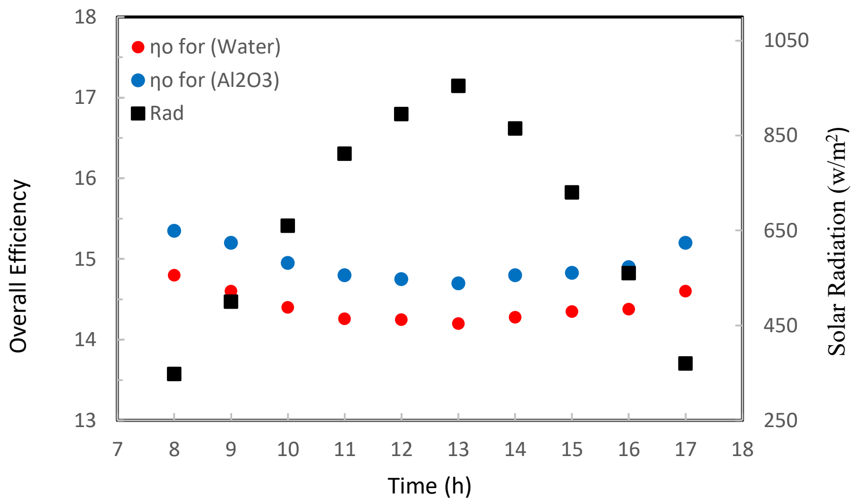

Fig. 8. Hourly variation of overall efficiency for the uncooled PV module, water-cooled PV/T collector and Al_2O_3/water nanofluid-cooled PV/T collector during a clear day in March 2025

Rys. 8. Zmiany ogólnej sprawności w ujęciu godzinowym dla modułu fotowoltaicznego bez chłodzenia, kolektora fotowoltaiczno-termicznego chłodzonego wodą oraz kolektora fotowoltaiczno-termicznego chłodzonego nanofluidem Al_2O_3/woda w pogodny dzień w marcu 2025 r.

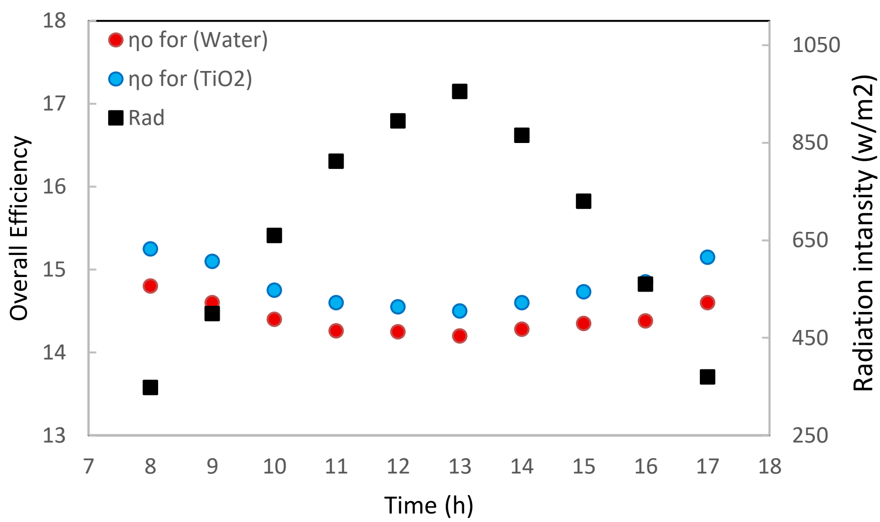

Fig. 9. Hourly variation of overall efficiency for the PV/T collector operated with water and TiO_2/water nanofluid, together with the corresponding solar radiation intensity

Rys. 9. Zmiany ogólnej sprawności w poszczególnych godzinach dla kolektora PV/T zasilanego wodą oraz nanofluidem TiO_2/woda, wraz z odpowiadającym im natężeniem promieniowania słonecznego

5. Validation with literature

The present results are in good agreement with previous studies on nanofluid-cooled PV/T collectors and provide new field-scale evidence under extreme heat conditions. The Al_2O_3/water coolant effectively reduced the PV cell temperature by about 28°C, lowering it from approximately 60°C for the air-cooled panel to around 30–32°C. This strong cooling capability demonstrates stable thermal regulation under the high irradiance levels of Kirkuk (March 2025). The magnitude of ΔT obtained in this work is comparable to, or slightly higher than, reductions reported for Al_2O_3-based coolants in moderate-climate or laboratory studies summarized in Table 1. This gain is attributed to the combination of high solar flux with the spiral-tube heat-exchanger geometry, which provides higher convective heat transfer compared to flat-plate or serpentine geometries.

For electrical efficiency, the nanofluid-cooled PV/T can increase from 12.3% (PV) up to approximately 13.9%, while the water-cooled PV/T system is at 13.6%. The increase of +1.6% deltaPV from the baseline PV is in line with other published values for Al_2O_3 nanofluids, and the fact that it was achieved outdoors on an operational PV system vs. an experiment-controlled environment is highly noteworthy. From a mechanical perspective, such enhancement is consistent with the known dependence of low cell temperature on higher open-circuit voltage and maximum power output. The outcome further supports the previously reported literature regarding effective heat removal leading to better PV performance.

For thermal effectiveness, the range of 12–20% (average 16%) found is believable for a midday hot case, constant flow rate, and spiral-tube arrays examined. While some of the optimized flat-plate or hybrid-channel systems in the literature present marginally higher peak efficiencies, they are usually obtained with mild weather and hydraulic parameter tuning. The current results can be considered as a conservative but realistic baseline for spiral-tube collectors with PV/T absorber components under high heat flux conditions, which still holds significant room for improvement through flow rate optimization or internal channel augmentation.

The overall system performance was also shown to be enhanced by 15.2% with the nanofluid-based PV/T system compared to 14.4% for the water-cooled setup. This increase of +0.8% points is a result of the combined electrical and thermal gains, demonstrating the net system-level gain from using Al_2O_3/water as active coolant. Altogether, the strong temperature suppression, continuous electrical enhancement, and constant thermal behavior revealed that nanofluid cooling is an efficient approach to boosting PV/T collector performance under hot climate conditions. These results are consistent with previous works, and the previous studies were extended by extending their conclusion to an outdoor spiral-tube configuration under extreme heat.

6. Limitations and future work

The current study has several limitations, which must be recognized. First, the tests were carried out only in March 2025, and this limitation implies that the analysis was done using results within/for a single testing period and does not consider seasonal variations of solar radiation and ambient temperature. Second, the effect of only one type (Al_2O_3/water) and a concentration level (0.5 wt%) of nanofluid has been studied. Different nanofluids like ZnO, CuO, TiO_2, or hybrid mixtures and different concentration levels may lead to differences in thermal/electric properties. Third, the device was characterized for a single mass flow rate and for one specific configuration of the spiral tube. This restricts the applicability of the findings to different hydraulic and geometric conditions. Lastly, the economical and environmentally friendly aspect of nanofluid preparation and pumping power demand, or long-term operational stability was not taken into account.

It is, thus, necessary for future studies to expand the range of the working envelope to map the performance trend under broader ranges of conditions. In particular, tests in other nanofluid concentrations (e.g., 0.2 wt% and 0.5 wt%) and different mass flow rates away from the current set-point would contribute to providing insight into the trade-off between the improvement in heat transfer and hydraulic costs. Seasonal or prolonged trials are further advised to record variations in irradiance, ambient temperature, and nanoparticle stability. This work is designed to (i) determine how ΔT_{cell} and electrical efficiency scale with concentration; (ii) identify a range of flow rates that maximizes thermal efficiency without excessive pumping losses, and (iii) provide field-relevant boundaries for overall efficiency under both mild and extreme climatic conditions.

Moreover, techno-economic and life-cycle analyses should be performed to assess the large-scale applicability of nanofluid-cooled spiral-tube PV/T collectors in a hot dry climate. It is only fitting that such a test, or device for performing it, takes into consideration the cost of nanoparticles, fluid preparation and maintenance, and environmental considerations.

Conclusions

The present investigation provides clear experimental evidence that integrating an Al_2O_3/water nanofluid with a spiral-tube PV/T collector can substantially enhance system performance under the hot semi-arid climate of Kirkuk. Under peak irradiance, the nanofluid-cooled configuration lowered the PV cell temperature to around 29°C (compared with about 35°C for water cooling and 60°C for the uncooled module) and delivered higher electrical, thermal, and overall efficiencies, confirming the technical merit of nanofluid-based cooling for rooftop PV/T applications in harsh environments. The side-by-side outdoor testing of uncooled, water-cooled and nanofluid-cooled systems under identical conditions isolates the specific contribution of the spiral-tube geometry and the Al_2O_3/water nanofluid, providing a consistent basis for comparison with future designs. Although TiO_2/water was also examined as an alternative coolant and showed performance gains over water, Al_2O_3/water offered the most advantageous balance between enhanced thermal conductivity, manageable viscosity and short-term stability, and therefore emerges as the preferred working fluid within the operating range considered in this study.

This research was not funded by any grant.

The Authors have no conflicts of interest to declare.

References

Abdullah, M.S. and Hussein, A.M. 2023. Impact of coil pitch on heat transfer enhancement of a turbulent flow of α-Al_2O_3/DW nanofluid through helical coils. *Thermal Science* 27(6B), pp. 5005–5014, https://doi.org/10.2298/TSCI230227131A.

Abid et al. 2025 – Abid, H.N., Nayef, U.M., Mutlak, F.A.H., Muslim, A.M. and Muayad, M.W. 2025. Synthesis of Fe_3O_4 NPs on porous silicon for photoluminescence-based humidity sensor. Plasmonics 20, pp. 11773–11786, https://doi.org/10.1007/s11468-025-03250-7.

Akrouch et al. 2023 – Akrouch, M.A., Chahine, K., Faraj, J., Hachem, F., Castelain, C. and Khaled, M. 2023. Advancements in cooling techniques for enhanced efficiency of solar photovoltaic panels: A detailed comprehensive review and innovative classification. *Energy and Built Environment* 6(2), pp. 248–276, https://doi.org/10.1016/j.enbenv.2023.11.002.

Alhussen, A.Y. and Hussein, A.M. 2024a. Availability prediction of a double-pipe exchanger using twisted tape and nanofluid (Al_2O_3) technology. *Global Journal of Research in Engineering and Computer Sciences* 4(6), pp. 57–73, https://doi.org/10.5281/zenodo.14211275.

Alhussen, A.Y. and Hussein, A.M. 2024b. Availability prediction of a double pipe heat exchanger using twisted tape and nanofluids. *International Journal of Heat and Technology* 42(5), https://doi.org/10.18280/ijht.420516.

Awad, A. and Hussein, A. 2024. Influence of nanofluid types on the enhancements of solar collector performance. *International Innovations Journal of Applied Science* 1(2), https://doi.org/10.61856/f7m6ty09.

Awad, A.T. and Muayad, M.W. 2023. Experimental heat transfer study of an enhanced storage medium. *Journal of Energy Storage* 73(A), https://doi.org/10.1016/j.est.2023.108953.

Awad et al. 2021 – Awad, A., Ahmed, W. and Waleed, M. 2021. *Nanotechnology for energy storage*. [In:] *Emerging nanotechnologies for renewable energy*, pp. 495–516, https://doi.org/10.1016/B978-0-12-821346-9.00009-2.

Awad et al. 2025 – Awad, A.T., Taifor, M.N., Yaseen, A.H., Nayef, U.M., Abeda, T.H., Muayad, M.W. and Wen, D. 2025. Enhanced energy storage via one-step preparation of Cuo-nanosalt. *The European Physical Journal Plus* 140(10), https://doi.org/10.1140/epjp/s13360-025-06924-7.

Aydın et al. 2022 – Aydın, A., Kayri, İ. and Aydin, H. 2022. Determination of the performance improvement of a PV/T hybrid system with a novel inner plate-finned collective cooling with Al_2O_3 nanofluid. *Energy*

Sources, Part A: Recovery, Utilization and Environmental Effects 44(4), pp. 9663–9681, https://doi.org/10.1080/15567036.2022.2136801.
Dubey, S. and Tiwari, G.N. 2008. Thermal modeling of a combined system of photovoltaic thermal (PV/T) solar water heater. *Solar Energy* 82(7), pp. 602–612, https://doi.org/10.1016/j.solener.2008.02.005.
Einstein, A. 1906. A new determination of molecular dimensions. *Annalen der Physik* 19, pp. 289–306.
Eisapour et al. 2020 – Eisapour, M., Eisapour, A.H., Hosseini, M.J. and Talebizadehsardari, P. 2020. Exergy and energy analysis of wavy tubes photovoltaic-thermal systems using microencapsulated PCM nano-slurry coolant fluid. *Applied Energy* 266, https://doi.org/10.1016/j.apenergy.2020.11484.
Faheem et al. 2024 – Faheem, M., Abu Bakr, M., Ali, M., Majeed, M.A., Haider, Z.M. and Khan, M.O. 2024. Evaluation of efficiency enhancement in photovoltaic panels via integrated thermoelectric cooling and power generation. *Energies* 17(11), https://doi.org/10.3390/en17112590.
Ghadikolaei, S.S.C. 2021. Solar photovoltaic cells performance improvement by cooling technology: An overall review. *International Journal of Hydrogen Energy* 46(18), pp. 10939–10972, https://doi.org/10.1016/j.ijhydene.2020.12.164.
Hameed et al. 2024 – Hameed, M.A., Hussein, A.M. and Awad, A.T. 2024. Solar collectors with nanofluid for domestic applications: A review. *NTU Journal of Renewable Energy* 7(1), pp. 57–64, https://doi.org/10.56286/dskpxb94.
Hasan et al. 2025 – Hasan, F.H., Algburi, S. and Ezzat, S.B. 2025. Investigating the impact of internal and external factors on solar cell performance to enhance energy conversion efficiency. *NTU Journal of Renewable Energy* 8(1), pp. 14–23, https://doi.org/10.56286/x12hd434.
Hissouf et al. 2020 – Hissouf, M., Feddaoui, M., Najim, M. and Charef, A. 2020. Numerical study of a covered photovoltaic-thermal collector (PVT) enhancement using nanofluids. *Solar Energy* 199, pp. 115–127, https://doi.org/10.1016/j.solener.2020.01.083.
Hosouli et al. 2024 – Hosouli, S., Gaikwad, N., Qamar, S.H. and Gomes, J. 2024. Optimizing photovoltaic thermal (PVT) collector selection: A multi-criteria decision-making (MCDM) approach for renewable energy systems. *Heliyon* 10(6), https://doi.org/10.1016/j.heliyon.2024.e27605.
Ibrahim et al. 2023 – Ibrahim, A., Ramadan, M.R., Khallaf, A.E.-M. and Abdulhamid, M. 2023. A comprehensive study for Al_2O_3 nanofluid cooling effect on the electrical and thermal properties of polycrystalline solar panels in outdoor conditions. *Environmental Science and Pollution Research* 30(49), pp. 106838–106859, https://doi.org/10.1007/s11356-023-25928-3.
Jia et al. 2020 – Jia, Y., Ran, F., Zhu, C. and Fang, G. 2020. Numerical analysis of photovoltaic-thermal collector using nanofluid as a coolant. *Solar Energy* 196, pp. 625–636, https://doi.org/10.1016/j.solener.2019.12.069.
Kalogirou et al. 2016 – Kalogirou, S.A., Karellas, S., Badescu, V. and Braimakis, K. 2016. Exergy analysis on solar thermal systems: A better understanding of their sustainability. *Renewable Energy* 85, pp. 1328–1333, https://doi.org/10.1016/j.renene.2015.05.037.
Khaleel Rashid et al. 2025 – Khaleel Rashid, M., Mohammed, H.J., Hameed, H.M., Muayad, M.W., Hussien, A.M., Awad, A.T. and Alharbi, M. 2025. The effect of titanium dioxide (TiO_2) nanoparticle concentration on the performance of polycrystalline silicon solar cells. Journal of Umm Al-Qura University for Engineering and Architecture 16, pp. 1753–1764, https://doi.org/10.1007/s43995-025-00207-z.
Khlaief et al. 2025 – Khlaief, J.H., Nayef, U.M., AbdulHussien, A.M. and Muayad, M.W. 2025. Synthesis of Au@CdO nanoparticles using laser ablation deposited on porous silicon for photodetector applications. *Optics & Laser Technology* 192, https://doi.org/10.1016/j.optlastec.2025.114072.
Lima-Téllez et al. 2024 – Lima-Téllez, T., Hinojosa, J.F., Hernández-López, I. and Moreno, S. 2024. Numerical study of the thermal performance of a single-channel cooling PV system using baffles and different nanofluids. *Heliyon* 10(15), https://doi.org/10.1016/j.heliyon.2024.e35413.

Maxwell, J.C. 2011. *An Elementary Treatise on Electricity*. Cambridge: Cambridge University Press.

Mohammed et al. 2024 – Mohammed, A.J., Ali, H.H.M., Barrak, A.S., Hussein, A.M. and Mohammed, M.R. 2024. Enhancement of turbulent heat transfer by using CuO nano-particle and twisted tape. *Pollack Periodica* 19(3), pp. 115–121, https://doi.org/10.1556/606.2024.00985.

Muayad, M.W., Nayef, U.M., Hadi, A.J., Ali, H.T., Hussein, A.M. and Awad, A.T. (2025) 'Synthesis of SnO_2 nanoparticles via laser ablation for high-performance photodetectors', Plasmonics, 1–12.

Murtadha, T.K. and Hussein, A.A. 2022. Optimization the performance of photovoltaic panels using aluminum-oxide nanofluid as cooling fluid at different concentrations and one-pass flow system. *Results in Engineering* 15, https://doi.org/10.1016/j.rineng.2022.100541.

Najim et al. 2022 – Najim, S.M., Hussein, A.M. and Danook, S.H. 2022. A review of performance enhancement of the shell and tube heat exchanger by using nanofluid. *AIP Conference Proceedings* 2398(1), https://doi.org/10.1063/5.0093740.

Pak, B.C. and Cho, Y.I. 1998. Hydrodynamic and heat transfer study of dispersed fluids with submicron metallic oxide particles. *Experimental Heat Transfer* 11(2), pp. 151–170.

Pathak et al. 2022 – Pathak, S.K., Sharma, P.O., Goel, V., Bhattacharyya, S., Aybar, H.Ş. and Meyer, J.P. 2022. A detailed review on the performance of photovoltaic/thermal system using various cooling methods. *Sustainable Energy Technologies and Assessments* 51, https://doi.org/10.1016/j.seta.2021.101844.

Rahman et al. 2024 – Rahman, M.A., Hasnain, S.M.M., Pandey, S., Tapalova, A., Akylbekov, N. and Zairov, R. 2024. Review on nanofluids: Preparation, properties, stability, and thermal performance augmentation in heat transfer applications. *ACS Omega* 9(30), pp. 32328–32349, https://doi.org/10.1021/acsomega.4c03279.

Shaalan et al. 2025a – Shaalan, Z.A., Hussein, A.M., Abdullah, M.Z., Alsayah, A.M., Alshukri, M.J. and Khaled, M. 2025. Enhanced photovoltaic cooling using ZnO/TiO_2 hybrid nanofluids: Numerical and experimental analysis. *International Journal of Thermofluids* 27, https://doi.org/10.1016/j.ijft.2025.101222.

Shaalan et al. 2025b – Shaalan, Z.A., Hussein, A.M. and Abdullah, M.Z. 2025. Numerical-experimental study to improve photovoltaic panel cooling by using hybrid ZnO/Al_2O_3 nanofluids. *Case Studies in Thermal Engineering* 70, https://doi.org/10.1016/j.csite.2025.106053.

Srimanickam et al. 2025 – Srimanickam, B., Vandhana Devi, V., Muralidharan, K., Sarasu, P., Srividhya, S., Elangovan, K. and Krishnamoorthy, R. 2025. Experimental and machine learning evaluation of a solar PVT system with water and Al_2O_3 nanofluids for improved electrical and thermal efficiency. *Journal of Thermal Analysis and Calorimetry* 150, pp. 15649–15662, https://doi.org/10.1007/s10973-025-14589-8.

Wang et al. 2022 – Wang, X., Li, W., Luo, Z., Wang, K. and Shah, S.P. 2022. A critical review on phase change materials (PCM) for sustainable and energy efficient building: Design, characteristic, performance and application. *Energy and Buildings* 260, https://doi.org/ 10.1016/j.enbuild.2022.111923.

Mohammed Mahmood Mustafa, Adnan M. Hussein, Afrah Turki Awad

Poprawa wydajności kolektora PV/T z rurami spiralnymi dzięki zastosowaniu nanofluidu w gorącym klimacie: badania eksperymentalne

Streszczenie

W niniejszym badaniu eksperymentalnie zbadano wydajność kolektora fotowoltaiczno-termicznego (PV/T) z rurą spiralną, zintegrowanego z modułami fotowoltaicznymi z krzemu monokrystalicznego i chłodzonego za pomocą nanofluidu Al_2O_3/woda. Testy terenowe przeprowadzono w Kirkuku (Irak) w marcu 2025 r. w warunkach eksploatacyjnych. Jako płyn roboczy zastosowano nanofluid zawierający 0,5% mas. Al_2O_3, a jego wydajność porównano z wydajnością płaskich paneli fotowoltaicznych w warunkach chłodzenia powietrzem oraz nowoczesnych konfiguracji fotowoltaiczno-termicznych (PV/T) chłodzonych wodą. O godz. 13:00 kolektor chłodzony nanofluidem zdołał utrzymać ogniwo fotowoltaiczne w temperaturze minimalnej wynoszącej ~29°C, podczas gdy panele chłodzone wodą i powietrzem nagrzały się odpowiednio do około 35°C i 60°C. Tymczasem sprawność elektryczna w tym momencie wynosiła 13,4% dla systemu PV/T chłodzonego nanofluidem, 12,6% dla systemu z blokiem wodnym oraz 11,8% dla konwencjonalnego modułu fotowoltaicznego. Sprawność cieplna systemu PV/T z nanofluidem wynosiła około 13%, podczas gdy dla systemu wodnego wynosiła 12%. Należy również zauważyć, że sprawność netto osiągnęła ~15,1% w przypadku systemu z nanofluidem oraz 14,5% dla systemu chłodzonego wodą. Wyniki wskazują, że chłodzenie nanofluidem skutecznie ogranicza wzrost temperatury ogniw fotowoltaicznych, zapewniając tym samym lepszą wydajność elektryczną, termiczną i ogólną w warunkach upałów w południe. W odróżnieniu od wcześniejszych badań przeprowadzonych w umiarkowanych warunkach pogodowych i dotyczących płaskich kolektorów PV/T niniejsze badanie eksperymentalnie wykazuje możliwość niezawodnej pracy kolektora PV/T z rurami spiralnymi, chłodzonego nanofluidem, w warunkach intensywnego upału panującego w Iraku.

Słowa kluczowe: PV/T, kolektor z rurami spiralnymi, nanofluid Al_2O_3, wydajność chłodnicza PV